Surface Modification of a Doped BaCeO₃ to Function as an Electrolyte and as an Anode for SOFCs

Atsuko Tomita,[a] Takashi Hibino,[b,*,z] and Mitsuru Sano[b]

[a]*Materials Research Institute for Sustainable Development, National Institute of Advanced Industrial Science and Technology, Moriyama-ku, Nagoya 463-8560, Japan*
[b]*Graduate School of Environmental Studies, Nagoya University, Chikusa-ku, Nagoya 464-8601, Japan*

Dual functions of $BaCe_{0.8}Y_{0.2}O_{3-\alpha}$ (BCY) as an electrolyte and as an anode were improved for solid oxide fuel cell (SOFC) applications. A porous Ce-rich phase with fluorite structure was formed with a depth of ~ 10 μm from the BCY surface by vaporization of BaO from the BCY surface at 1700°C. The resulting BCY surface showed enough electronic conductivity to provide electrical collection and a high electrocatalytic activity for hydrogen oxidation. A hydrogen-air fuel cell with the BCY electrolyte exhibited reasonable performances without using an anode material between 750 and 950°C.
© 2005 The Electrochemical Society. [DOI: 10.1149/1.1928230] All rights reserved.

Ni/yttria-stabilized zirconia (YSZ) cermet is the most commonly used anode in solid oxide fuel cells (SOFCs). While the Ni/YSZ cermet electrodes have excellent electrocatalytic properties for internal reforming or direct oxidation of hydrocarbons, they promote coking, causing a serious carbon deposition on the anode surface. Furthermore, the Ni/YSZ cermet electrodes suffer from volume change upon redox cyclings when SOFC systems are stopped and restarted. Such disadvantages are the main reasons for long-term degradation of SOFCs, especially operating in the intermediate-temperature range (600–800°C). In recent years, CeO_2, $Zr_{1-x-y}Ti_xY_yO_2$, $LaCrO_3$- or $SrTiO_3$-based materials have been proposed as alternative anodes.[1] These materials are required to display many characteristic properties in addition to the resistance to carbon deposition and the stability to redox cycling: mixed electron- and oxide-ion conductivity, catalytic reactivity for fuel oxidation, chemical stability, compatible thermal expansion, and mechanical strength. On the other hand, we have attempted to develop a single material functioning as both an electrolyte and anode (hereafter referred to as the electrochemical dual-functioning material, EDFM).[2] Because the EDFM essentially meets the mechanical criteria for an electrode (*i.e.*, thermal expansion and mechanical strength), it may more successfully overcome the above disadvantages. It was found in a previous study[2] that the most suitable material for this purpose was doped $BaCeO_3$, notably $BaCe_{0.76}Y_{0.20}Pr_{0.04}O_{3-\alpha}$, which showed an open-circuit voltage of more than 1000 mV and a peak power density of 61 mW cm^{-2} (electrolyte thickness was 0.5 mm) without the need for anode material at 800°C. However, the fuel cell still showed a high internal resistance, with ohmic resistance at 2.13 Ω cm^2 and polarization resistance at 1.16 Ω cm^2. A further reduction in internal resistance would make this EDFM a promising alternative to the Ni/YSZ cermet.

In this study, we focused on the vaporization of BaO from the doped $BaCeO_3$ surface at high temperatures (1500–1700°C)[3]

$$BaCe_{1-x}M_xO_{3-\alpha} \rightarrow BaO(g) + Ce_{1-x}M_xO_{2-x/2} \qquad [1]$$
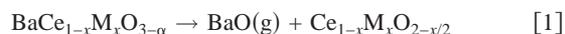
where M are trivalent cations such as Y^{3+}. ($Pr^{3+,4+}$ cannot be used as a dopant cation here because the vapor pressure of Pr_xO_y is relatively high in the temperature range of interest.) As a result, a Ce-rich phase can be expected to be formed over the external surface of the electrolyte, which may decrease the interfacial contact resistance between the electrolyte and interconnect by reducing Ce^{4+} to Ce^{3+} at the fuel side of the electrolyte. This reduction may also promote the anode reaction on the electrolyte surface. In addition, the Ce-rich phase offers the possibility of acting as a protection layer against CO_2 included in the fuel gas, leading to an improvement in the

chemical stability of the electrolyte; $BaCeO_3$ thermodynamically reacts with CO_2 below 1200°C according to[4]

$$BaCeO_3 + CO_2 \rightarrow BaCO_3(=BaO + CO_2(g)) + CeO_2 \qquad [2]$$
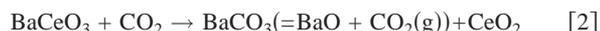
The objective of the present paper was therefore to improve a Y-doped $BaCeO_3$ by heat-treatment and to examine the performances of an SOFC with the obtained EDFM.

Experimental

The Y-doped $BaCeO_3$ used in this study was $BaCe_{0.8}Y_{0.2}O_{3-\alpha}$ (BCY). The preparation of this material has been described in detail elsewhere.[5] The BCY ceramic was cut into a disk (14 mm diam, *ca.* 1 mm thick) and then polished to a thickness of 0.5 mm with an abrasive paper with an average particle size of 25 μm. The disk was heated between 1500 and 1700°C for 10 h in air to vaporize BaO existing in the vicinity of the disk surface. Changes in the disk surface after heating were characterized by X-ray diffraction (XRD) and scanning electron microscopy (SEM) techniques coupled to an energy dispersive X-ray (EDX) detector. A commercial Pt paste (Tokuriki) was painted as the cathode on the surface (0.5 cm^2 area) with ethyl carbitol as a solvent, followed by heating at 950°C in air for 1 h. Another surface (fuel side) was not treated at all, where an Au net (100 MESH) was simply placed for electrical collection. A Pt reference electrode was deposited by painting the Pt paste on the surface of the side (*ca.* 0.1 cm^2) of the disk and then heating at 950°C in air for 1 h. Two gas chambers were set up by placing the cell between two alumina tubes. Each chamber was sealed by melting a glass ring gasket at 950°C. The fuel and air chambers were supplied with wet hydrogen, which was saturated with water vapor at room temperature, and atmospheric air, respectively, at a flow rate of 30 mL min^{-1}. The reference electrode was statically exposed to atmospheric air. The current density-cell voltage curves and the impedance spectra were measured by the four probe method. The transport numbers of proton and oxide ion were analyzed by measuring the water vapor concentration in the outlet gases from the fuel and air chambers using a humidity sensor.[2,6] In this case, the water vapor concentration in both hydrogen and air at the inlet was controlled at 0.6%.

Results and Discussion

Figure 1 shows XRD patterns of the untreated and heat-treated BCY surfaces, which also includes the patterns of $Ce_{0.9}Gd_{0.1}O_{1.95}$ for comparison. The untreated BCY surface showed no other phases than the perovskite phase. For the heat-treated BCY surface, the diffraction signals of the perovskite phase became gradually smaller as the treatment temperature increased. In contrast, characteristic signals of the fluorite phase appeared, mainly at 28.7, 33.2, 47.7, and 56.5°, the intensity of which continuously increased with increasing treatment temperature. No signals of the other phases were visible for all the heat-treated BCY surfaces. These changes can be ex-
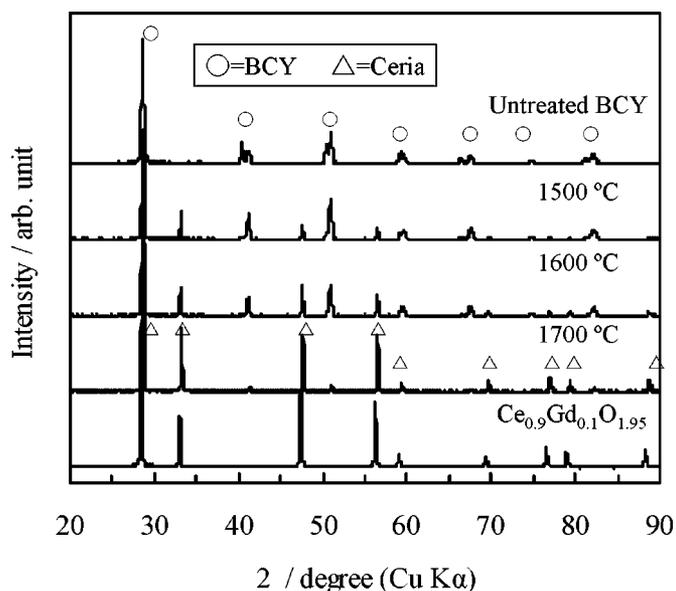
Figure 1. XRD patterns of untreated and heat-treated BCY surfaces. The heat treatment was made in the range of 1500–1700°C. The patterns of $Ce_{0.9}Gd_{0.1}O_{1.95}$ are also included for comparison.

Figure 3. Dependence of electrical conductivity for untreated and heat-treated BCY half-cells on partial pressure of oxygen at 800°C. The data were obtained by depositing a Pt working electrode on each BCY surface, followed by measuring the electrical resistance through the Pt reference electrode in different atmospheres.

pected to result from the proposed Reaction 1. Because we would like to form as much Ce-rich phase as possible over the BCY surface, the BCY disk heat-treated at 1700°C was used in subsequent experiments.

The cross-sections of the untreated and heat-treated BCY disk are shown in Fig. 2. The SEM images revealed that the heat-treated BCY surface became porous and showed a significant increase in surface roughness, probably due to vigorous vaporization of BaO from the BCY surface. In a previous study,[2] we found that the polarization resistance at the fuel side of the EDFM was reduced with increasing surface roughness, which suggests that the increase in surface roughness for the BCY disk by heat-treatment may promote the anode reaction (as described later). The EDX mapping for the heat-treated BCY surface showed a much lower elementary distribution of Ba than of Ce and Y at a depth of ~10 μm from the surface. In addition, there were no large differences in Ce and Y concentrations between the surface and bulk compositions. Therefore, the Ce-rich phase is considered to have a composition near $Ce_{0.8}Y_{0.2}O_{1.9}$.

To investigate the electrochemical properties of the Ce-rich phase formed over the BCY surface, we deposited a Pt working electrode on its surface and measured the half-cell resistance through the reference electrode. Here, it should be noted that the obtained results reflect the nature not only of the Ce-rich phase, but also of the BCY bulk between the working and reference electrodes.
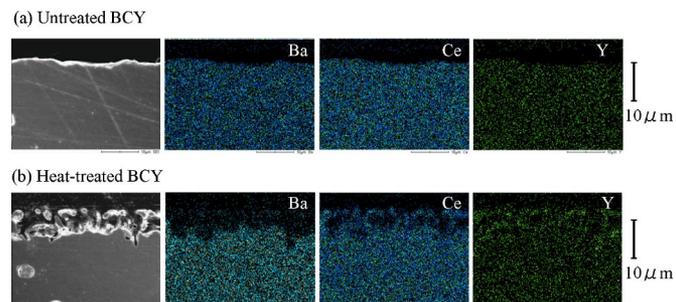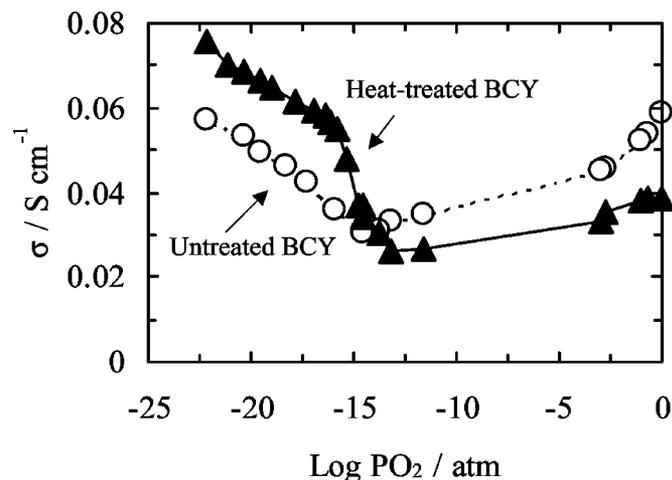

Figure 2. SEM and EDX observations of (a) untreated and (b) heat-treated BCY disks.

Figure 3 shows the dependence of the electrical conductivity for the untreated and heat-treated BCY half-cells on the partial pressure of oxygen at 800°C. For the untreated BCY half-cell, reducing oxygen partial pressure resulted in a transition from dominant p-type electronic to ionic conduction, followed by n-type electronic conduction. The reduction of Ce^{4+} to Ce^{3+} in $BaCe_{0.85}Y_{0.15}O_{3-\alpha}$ at low partial pressures of oxygen has recently been reported by Kruth *et al.*[7] On the other hand, a large increase in the conductivity with decreasing oxygen partial pressure was observed for the heat-treated BCY half-cell, indicating that the heat-treated BCY is more significantly reduced than the untreated BCY. We note that such a significant reduction is limited to the Ce-rich phase formed over the BCY surface; the BCY bulk is not subjected to serious reduction. Indeed, the half-cell potential with the heat-treated BCY was 1020 mV when the partial pressures of oxygen at the working and reference electrodes were 10^{-24} and 0.21 atm, respectively. However, there appears to be a question how just a 10 μm thick Ce-rich phase caused the large increase in conductivity of the heat-treated BCY shown in Fig. 3. Although we cannot give a clear explanation at the present stage, it may be suggested that the appearance of n-type electron conduction in the Ce-rich phase substantially reduces the contact resistance between the electrolyte and electrode that occupies some fractions of the total ohmic resistance. On the other hand, Fig. 4 shows the anodic polarization resistance between the Pt working electrode and the untreated or heat-treated BCY electrolyte in hydrogen at different temperatures. The polarization resistances with the heat-treated BCY electrolyte were lower than those with the untreated BCY electrolyte at all the tested temperatures. It is sufficient here to indicate that the Ce-rich phase has a higher electrocatalytic activity for the anode reaction of hydrogen or chemical surface exchange coefficient than the BCY surface. As described above, the Ce-rich phase grew in porous form over the BCY surface, probably resulting in an increase of the effective surface area. In addition, it is well known that CeO_2-based compounds are good catalysts for the oxidation of reducing gases, which may be applied to the present case.[8]

Two hydrogen-air fuel cells with the untreated and heat-treated BCY electrolytes were fabricated without using an anode material. The discharge properties of the two fuel cells between 750 and 950°C are shown in Fig. 5. The open-cell voltages (OCVs) ranged from 940 to 1058 mV for both fuel cells, which are somewhat lower than the theoretical values of 1076 to 1110 mV. The difference between the theoretical and measured values is mainly attributed to
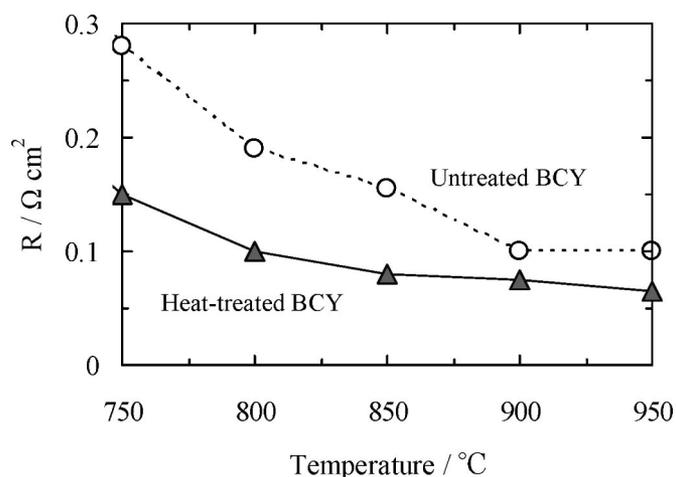
Figure 4. Polarization resistance for untreated and heat-treated BCY half-cells in hydrogen at different temperatures. The data were obtained using the same half-cells as those shown in Fig. 3. The impedance spectra were measured by changing the frequency from 0.1 to 100 kHz.

either electron or electron-hole conduction in the BCY electrolyte, as shown in Fig. 3. A comparison between the fuel cells indicated that the present heat treatment largely improved the fuel-cell performance. The impedance spectra for the two fuel cells further clarified this point; the polarization resistance decreased from 2.33 to 0.84 Ω cm^2 at 800°C, although the ohmic resistance was not much influenced by heat treatment. This is evidently due to the increase in electrical path for current collection (see Fig. 3) and in electrocatalytic activity for hydrogen oxidation (see Fig. 4) by the Ce-rich phase formed over the BCY surface.
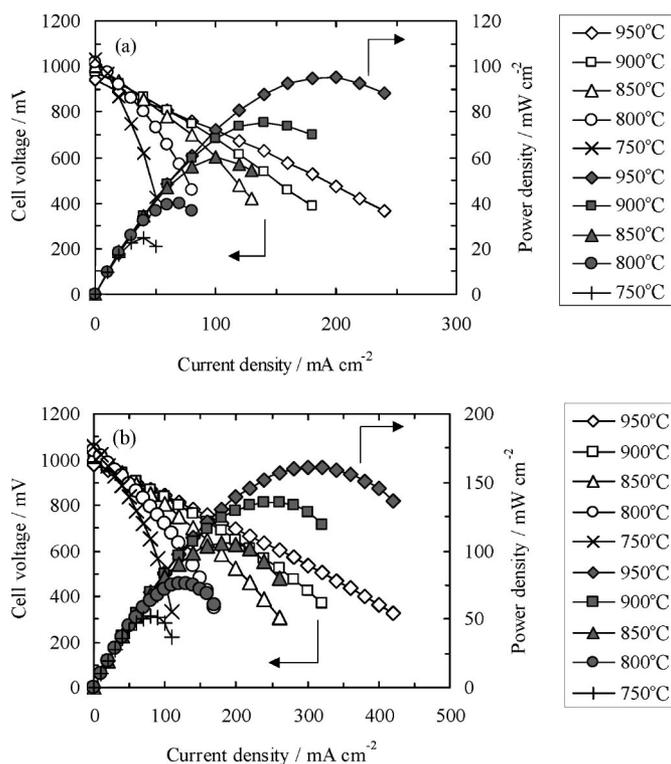

Figure 5. Discharge properties of SOFCs with (a) untreated and (b) heat-treated BCY electrolytes between 750 and 950°C. The SOFCs were operated without using an anode material.
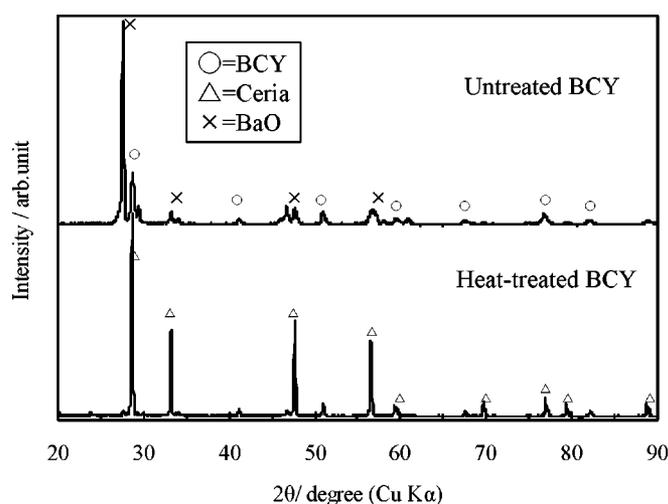

Figure 6. XRD patterns of the untreated and heat-treated BCY surfaces after exposure to CO_2 at 950°C. CO_2 treatment was made by exposing the samples to a mixture of 50 vol % CO_2 and 50 vol % Ar at 950°C and 30 mL min^{-1} for 1 h.

Because protons and oxide ions serve as the charge carriers in $BaCeO_3$-based electrolytes,[5,6,9] we evaluated the transport numbers of proton and oxide ion in the untreated and heat-treated BCY electrolytes using the two SOFCs shown in Fig. 5. The measurement of the formation rate of water vapor at the anode and cathode during cell discharge is useful for this purpose. In general, oxide-ion conducting electrolytes such as YSZ produce water vapors at the anode through Reaction 3. However, when the electrolyte shows mixed proton- and oxide-ion conduction, water vapors are produced not only at the anode but also at the cathode according to Reaction 4

Anode $\qquad\qquad O^{2-} + H_2 \rightarrow H_2O + 2e^-$ $\qquad$ [3]

Cathode $\qquad\qquad 2H^+ + 1/2\ O_2 + 2e^- \rightarrow H_2O$ $\qquad$ [4]
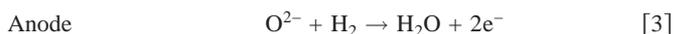
In this case, the ion transport number can be determined from the ratio of the formation rate of water vapor at the cathode for protons and at the anode for oxide ions to the total formation rates of water vapor calculated from Faraday's law. For the heat-treated BCY electrolyte, water vapor was more strongly evolved at the cathode than at the anode at 800°C, indicating that proton conduction is more predominant than oxide-ion conduction under the present conditions. The proton transport number was calculated to be in the range of 0.65 to 0.75, which was higher than the proton transport number of 0.45 to 0.50 observed for the untreated BCY electrolyte. This preponderance of proton conduction can be related to the reduction in anodic polarization resistance by the Ce-rich phase. Put another way, the anodic reaction of protons more easily proceeds on the heat-treated BCY surface than on the untreated BCY surface, thus bringing about a relatively higher proton transport number in the heat-treated BCY electrolyte.

We finally verified whether the Ce-rich phase acts as a protective layer against CO_2. The XRD patterns of the untreated and heat-treated BCY surfaces after exposure to CO_2 at 950°C for 1 h are shown in Fig. 6. The heat-treated BCY surface did not react with CO_2, while the untreated BCY surface was decomposed to BaO and CeO_2. After the experiments, the former surface remained almost unchanged, but the latter surface turned white. These results indicate that the Ce-rich phase provides a high tolerance to CO_2 for the BCY surface. This is because the reaction of CeO_2 with CO_2 is thermodynamically impossible. One can also expect that a similar effect of the Ce-rich phase on the stability to CO_2 is available to every application (conventional SOFCs, chemical sensors, and membrane reactors) using $BaCeO_3$-based electrolytes.

In conclusion, the present results demonstrate that the performance of the BCY-based EDFM for SOFCs can be largely improved by heat-treatment. However, additional research still has to be done to further enhance potential applicability of the EDFM for this type of SOFC. We are now investigating the stability of the heat-treated BCY electrolyte to redox and thermal cyclings and its resistance to carbon deposition. In addition, the use of a thin BCY film is needed to minimize the ohmic resistance of the electrolyte. (In this study, a BCY electrolyte with a thickness of 0.5 mm was used.) Finally, the development of a more inexpensive current collector than the Au net is required for actual applications.

References

1. A. Atkinson, S. Barnett, R. J. Gorte, J. T. S. Irvine, A. J. Mcevoy, M. Mogensen, S. C. Singhal, and J. Vohs, *Nat. Mater.*, **3**, 17 (2004).
2. D. Hirabayashi, A. Tomita, M. E. Brito, T. Hibino, U. Harada, M. Nagao, and M. Sano, *Solid State Ionics*, **168**, 23 (2004).
3. T. Matsui, *Thermochim. Acta*, **253**, 155 (1995).
4. S. M. Haile, B. J. Wuensch, and T. Siegrist, *Solid State Ionics*, **125**, 355 (1999).
5. T. Hibino, A. Hashimoto, M. Suzuki, and M. Sano, *J. Electrochem. Soc.*, **149**, A1503 (2002).
6. H. Iwahara, T. Yajima, T. Hibino, and H. Ushida, *J. Electrochem. Soc.*, **140**, 1687 (1993).
7. A. Kruth and J. T. S. Irvine, *Solid State Ionics*, **162–163**, 83 (2003).
8. P. J. Gellings and H. J. M. Bouwmeester, *Catal. Today*, **58**, 1 (2000).
9. N. Bonanos, K. S. Knight, and B. Ellis, *Solid State Ionics*, **79**, 161 (1995).